

STRUCTURAL RELIABILITY OF LEG-SUPPORTED LIQUID
CONTAINERS UNDER A RANDOM EARTHQUAKE-TYPE
EXCITATION

By

Takafumi FUJITA^{I)}

SYNOPSIS

This paper deals with the structural reliability of leg-supported liquid containers subjected to a random earthquake-type excitation which is a nonstationary Gaussian shot noise. The system considered is a model for cylindrical or rectangular tanks supported by short legs. Employing a simple dynamical model which describes motion of the tank, stochastic analysis is carried out for the response of the system. The reliability is evaluated from the point of view of fatigue failure at such critical portions as connections between the tank shell and the supporting legs or anchored lower ends of the legs.

DYNAMICAL MODEL OF LEG-SUPPORTED LIQUID CONTAINERS

We consider a dynamical model for leg-supported liquid containers such as shown in Fig. 1.

VIBRATION CHARACTERISTICS: Figure 2 is an experimental result obtained by sinusoidal excitations of an experimental model with a rectangular tank (280 x 380 x 490^h). This figure shows the response factor on the displacement of the tank. Similar result is obtained for an experimental model with a cylindrical tank (470 ϕ x 485^h). As we can see from Fig. 2, the tank displacement due to sloshing of liquid can be neglected for not so huge tanks, which, in Fig. 2, is indicated by a small peak at 1.6 Hz, and the system behaves as if it were a single-degree-of-freedom (SDF) system. In addition, it is found that the system has a nonlinear damping caused by liquid in the tank.

ANALYSIS OF HARMONIC RESPONSE: In order to clarify the reason why only one eigen-frequency becomes dominant and the system behaves like a SDF system, the analysis based on the potential theory in fluid mechanics is carried out for the response of the system to

I) Associate Professor, Institute of Industrial Science,
University of Tokyo

sinusoidal excitation. In the analysis, the system is assumed to have no damping.

In the case of rectangular tanks, the response factor on the tank displacement is obtained as follows:

$$\left| \frac{X}{a} \right| = \left| \frac{k}{k - (m_0 + M_l) \omega_f^2 - \frac{\rho B D^3}{g} \left[\sum_{n=1}^{\infty} \left\{ \frac{8 \omega_f^4}{(2n-1)^4 \pi^4 (\Omega_n^2 - \omega_f^2)} \right\} + \frac{\omega_f^4}{12} \right] } - 1 \right|, \quad (1)$$

where X , a are amplitudes of the relative displacement of the tank and the forced sinusoidal displacement respectively; ω_f is the circular frequency of the forced displacement; k is the spring constant of the system; m_0 , M_l are, respectively, the mass of the system without liquid and the mass of liquid; ρ is the density of liquid; D , B are the length of a rectangular tank parallel to the exciting direction and the other length respectively; g is the acceleration of gravity; Ω_n is the eigen circular frequency of sloshing of the n -th order given by

$$\Omega_n = \sqrt{(2n-1) \pi \frac{g}{D} \tanh \left\{ (2n-1) \pi \frac{H}{D} \right\}} \quad (n=1, 2, \dots), \quad (2)$$

and where H is the depth of liquid. Likewise in the case of cylindrical tanks, the following equation is obtained:

$$\left| \frac{X}{a} \right| = \left| \frac{k}{k - (m_0 + M_l) \omega_f^2 - \frac{\rho \pi R^4}{g} \left[\sum_{n=1}^{\infty} \left\{ \frac{2 \omega_f^4}{\lambda_n^2 (\lambda_n^2 - 1) (\Omega_n^2 - \omega_f^2)} \right\} + \frac{\omega_f^4}{4} \right] } - 1 \right|, \quad (3)$$

where R is the radius of the tank; λ_n ($0 < \lambda_1 < \lambda_2 < \dots$) are roots of $J'_1(r) = 0$; Ω_n is give by

$$\Omega_n = \sqrt{\lambda_n \frac{g}{R} \tanh \left(\lambda_n \frac{H}{R} \right)} \quad (n = 1, 2, \dots). \quad (4)$$

Figure 3 shows the numerical result of Eq. (1) which corresponds to the experimental result in Fig. 2. In Fig. 3, the theoretical resonance curve has many peaks which are very narrow except one. Comparing Fig. 3 with Fig. 2, we can understand that these very narrow peaks are not observed in actual phenomena and only one wide peak is physically realized. The eigen-frequency corresponding to the wide peak is called here the "dominant eigen-frequency".

A SIMPLE METHOD FOR THE DOMINANT EIGEN-FREQUENCY: We now consider the case of rectangular tanks. Eigen-frequencies of the system are obtained as roots of the algebraic equation,

$$k - (m_0 + M_\ell) \omega^2 = \frac{\rho B D^3}{g} \left(\sum_{n=1}^{\infty} \left\{ \frac{8 \omega^6}{(2n-1)^4 \pi^4 (Q_n^2 - \omega^2)} \right\} + \frac{\omega^4}{12} \right). \quad (5)$$

Figure 4 shows the numerical result of each side of Eq. (5) where the same values of parameters are used as in Fig. 3. In Fig. 4, the eigen-frequencies are obtained from the crossing points of a straight curve and a group of curves. Considering the meanings of Eq. (1) and Eq. (5), we can find that the dominant eigen-frequency is represented by the crossing point of the straight curve and almost straight portions of the group of curves. Then this fact leads to a simple method to calculate the dominant eigen-frequency as shown in Fig. 5, where straight portions of the group of curves are replaced by a straight curve derived through an approximate method. In the case of cylindrical tanks, the same method is applied for the dominant eigen-frequency. Therefore, in both cases, the dominant eigen-frequency is calculated by

$$\omega_* = \sqrt{\frac{k + \beta \rho S_f g}{m_0 + M_\ell - \alpha \rho S_f D}} = \sqrt{\frac{k + \beta \rho S_f g}{m_0 + \rho S_f (H - \alpha D)}}, \quad (6)$$

where S_f is the area of free surface of liquid and α , β are constants given by

$$\alpha = 0.272, \quad \beta = 0.0281 \text{ for rectangular tanks,}$$

$$\alpha = 0.236, \quad \beta = 2.31 \text{ for cylindrical tanks.}$$

NONLINEAR DYNAMICAL MODEL WITH SINGLE-DEGREE-OF-FREEDOM: Equation (6) indicates that the equivalent mass and the equivalent spring constant of the system are, respectively,

$$\left. \begin{aligned} m_* &= m_0 + M_\ell - \alpha \rho S_f D, \\ k_* &= k + \beta \rho S_f g. \end{aligned} \right\} \quad (7)$$

To construct the dynamical model, a model for nonlinear damping of the system is required. Assuming that the nonlinear damping is proportional to the square of the response velocity of the tank, then the equation of motion of the system subjected to sinusoidal excitation is written as

$$m_* \ddot{x} + c_0 \dot{x} + c_\ell |\dot{x}| \dot{x} + k_* x = m_* a \omega_f^2 \cos \omega_f t, \quad (8)$$

where c_0 is the damping constant of the system without liquid and c_ℓ is the coefficient of the nonlinear damping.

Using the method of equivalent linearization, Eq. (8) is solved approximately and the resonance curve is obtained. Figure

6 shows the resonance curve of the experimental model with the rectangular tank where the value of $c\ell$ is decided through experiments. The experimental data in Fig. 6 are the same in Fig. 2. Analytical results agree well with experimental results, hence it is concluded that the assumption on the nonlinear damping is reasonable though the general expression for $c\ell$ is unknown. In the case of cylindrical tanks, the same conclusion is obtained.

PROBABILISTIC ANALYSIS OF THE RESPONSE TO A RANDOM EARTHQUAKE-TYPE EXCITATION

EQUATION OF MOTION: It is assumed that the restoring force of the system can be approximated by a linear one even though the strain at a critical portion of the system exceeds the range of elasticity. Therefore, using the nonlinear SDF model mentioned above, the equation of motion of the system subjected to seismic excitation can be written as

$$\left. \begin{aligned} \ddot{x} + 2\zeta\omega_* \dot{x} + \frac{2\mu}{D} |\dot{x}| \dot{x} + \omega_*^2 x &= -\ddot{z} , \\ x(0) = \dot{x}(0) &= 0 \end{aligned} \right\} \quad (9)$$

where

$$2\zeta = c_0 / \sqrt{m_* k_*}, \quad 2\mu / D = c\ell / m_*$$

and \ddot{z} is the acceleration of earthquake ground motion. As a stochastic model of \ddot{z} , the following nonstationary Gaussian shot noise is employed:

$$\ddot{z}(t) = \sqrt{\phi(t)} n(t), \quad (10)$$

where $\sqrt{\phi(t)}$ is a slow varying deterministic function of time and $n(t)$ is a Gaussian white noise. Then,

$$\left. \begin{aligned} E[\ddot{z}(t)] &= 0, \\ E[\ddot{z}(t) \ddot{z}(t+\tau)] &= 2A \phi(t) \delta(\tau), \end{aligned} \right\} \quad (11)$$

where A is a constant, δ is Dirac's delta function and $E[\cdot]$ denotes an ensemble mean.

NONSTATIONARY JOINT PROBABILITY DENSITY FUNCTIONS FOR THE RESPONSE DISPLACEMENT AND VELOCITY: For the purpose of the analysis of reliability, we require the one-time and the two-time joint probability density functions for the response displacement and the response velocity.

The one-time joint probability density function (PDF) satisfies the Fokker-Plank equation,

$$\frac{\partial p}{\partial t} + \dot{x} \frac{\partial p}{\partial x} - \frac{\partial}{\partial \dot{x}} \left\{ (2\zeta\omega_* \dot{x} + \frac{2\mu}{D} |\dot{x}| \dot{x} + \omega_*^2 x) p \right\} - A\phi(t) \frac{\partial^2 p}{\partial \dot{x}^2} = 0, \quad (12)$$

$$p(x, \dot{x}, 0) = \delta(x) \delta(\dot{x}).$$

As an approximate solution of Eq. (12), we can assume the following Gaussian distribution because the nonlinearity of the system is weak:

$$p(x, \dot{x}, t) = \frac{1}{2\pi \sqrt{\sigma_x^2(t)\sigma_{\dot{x}}^2(t) - \kappa_{x\dot{x}}^2(t)}} \exp \left\{ -\frac{\sigma_{\dot{x}}^2(t)x^2 - 2\kappa_{x\dot{x}}(t)x\dot{x} + \sigma_x^2(t)\dot{x}^2}{2 \{ \sigma_x^2(t)\sigma_{\dot{x}}^2(t) - \kappa_{x\dot{x}}^2(t) \}} \right\}$$

$$= \frac{1}{2\pi \{ \det S(t) \}^{1/2}} \exp \left\{ -\frac{1}{2} x^T S^{-1}(t) x \right\}, \quad (13)$$

where

$$\sigma_x^2(0) = \kappa_{x\dot{x}}(0) = \sigma_{\dot{x}}^2(0) = 0,$$

$$x \triangleq (x, \dot{x})^T,$$

$$S(t) = E[xx^T] = \begin{pmatrix} \sigma_x^2(t) & \kappa_{x\dot{x}}(t) \\ \kappa_{x\dot{x}}(t) & \sigma_{\dot{x}}^2(t) \end{pmatrix}. \quad (14)$$

Equation (13) contains three unknown functions, i.e., $\sigma_x^2(t)$, $\kappa_{x\dot{x}}(t)$ and $\sigma_{\dot{x}}^2(t)$, which are determined by solving the system of differential equations,

$$\left. \begin{aligned} \frac{d}{dt} \sigma_x^2(t) &= 2\kappa_{x\dot{x}}(t), \\ \frac{d}{dt} \kappa_{x\dot{x}}(t) &= \sigma_{\dot{x}}^2(t) - 2\zeta\omega_* \kappa_{x\dot{x}}(t) - \frac{8}{\sqrt{2\pi}} \frac{\mu}{D} \kappa_{x\dot{x}}(t) \sigma_{\dot{x}}(t) - \omega_*^2 \sigma_x^2(t), \\ \frac{d}{dt} \sigma_{\dot{x}}^2(t) &= -4\zeta\omega_* \sigma_{\dot{x}}^2(t) - \frac{16}{\sqrt{2\pi}} \frac{\mu}{D} \sigma_{\dot{x}}^3(t) - 2\omega_*^2 \kappa_{x\dot{x}}(t) + 2A\phi(t). \end{aligned} \right\} \quad (15)$$

Equations (15) are obtained by employing the method of weighted residuals (the method of moment).⁽¹⁾

Likewise, the two-time joint PDF is also approximated by the Gaussian distribution,

$$p(x_1, \dot{x}_1, t_1; x_2, \dot{x}_2, t_2) = \frac{1}{(2\pi)^2 \{ \det \tilde{S}(t_1, t_2) \}^{1/2}} \exp \left\{ -\frac{1}{2} \tilde{x}^T \tilde{S}^{-1}(t_1, t_2) \tilde{x} \right\}, \quad (16)$$

where

$$\begin{aligned}
\tilde{x} &= (x_1, \dot{x}_1, x_2, \dot{x}_2)^T \\
\tilde{S}(t_1, t_2) &= E[\tilde{x}\tilde{x}^T] \\
&= \begin{bmatrix} \sigma_{x^2}(t_1) & \kappa_{x\dot{x}}(t_1) & \gamma_{xx}(t_1, t_2) & \gamma_{x\dot{x}}(t_1, t_2) \\ \kappa_{x\dot{x}}(t_1) & \sigma_{\dot{x}^2}(t_1) & \gamma_{\dot{x}x}(t_1, t_2) & \gamma_{\dot{x}\dot{x}}(t_1, t_2) \\ \gamma_{xx}(t_1, t_2) & \gamma_{\dot{x}x}(t_1, t_2) & \sigma_{x^2}(t_2) & \kappa_{x\dot{x}}(t_2) \\ \gamma_{x\dot{x}}(t_1, t_2) & \gamma_{\dot{x}\dot{x}}(t_1, t_2) & \kappa_{x\dot{x}}(t_2) & \sigma_{\dot{x}^2}(t_2) \end{bmatrix} \\
&\triangleq \begin{bmatrix} S(t_1) & B(t_1, t_2) \\ B^T(t_1, t_2) & S(t_2) \end{bmatrix}
\end{aligned} \tag{17}$$

The matrices $S(t_1)$, $S(t_2)$ are given by Eqs. (14), (15), hence the matrix $R(t_1, t_2)$ is required to determine the approximate two-time joint PDF. Here we introduce the linearized equation of Eq. (9),

$$\ddot{x} + 2\bar{\zeta}_*(t)\omega_* \dot{x} + \omega_*^2 x = -\ddot{z}, \tag{18}$$

where $\bar{\zeta}_*$ is the statistically equivalent critical damping ratio given by

$$\bar{\zeta}_*(t) = \zeta + \frac{4}{\sqrt{2\pi}} \mu \frac{\sigma_{\dot{x}}(t)}{D\omega_*}, \tag{19}$$

and, as shown by Eq. (19), becomes a function of time because of nonstationariness. Let $\Phi(t_2, t_1)$ ($t_2 \geq t_1$) be the transition matrix with respect to the state vector $x = (x, \dot{x})^T$ of Eq. (18). Using the transition matrix, then $R(t_1, t_2)$ is written as

$$R(t_1, t_2) = \begin{cases} S(t_1) \Phi^T(t_2, t_1) & \text{for } t_2 \geq t_1, \\ \Phi(t_1, t_2) S(t_2) & \text{for } t_1 \geq t_2, \end{cases} \tag{20}$$

where $\Phi(t_2, t_1)$ is approximated by

$$\Phi(t_2, t_1) \approx e^{-\omega_* \{ \xi(t_2) - \xi(t_1) \}} \begin{bmatrix} \cos \omega_* (t_2 - t_1) & \frac{1}{\omega_*} \sin \omega_* (t_2 - t_1) \\ -\omega_* \sin \omega_* (t_2 - t_1) & \cos \omega_* (t_2 - t_1) \end{bmatrix}, \tag{21}$$

and where $\xi(t)$ is defined by

$$\xi(t) \triangleq \int_0^t \bar{\zeta}_*(s) ds. \tag{22}$$

NONSTATIONARY PROBABILITY DENSITY FUNCTIONS FOR THE ENVELOPE OF THE RESPONSE DISPLACEMENT: Since the response displacement of the system is a typical narrow-band random process, it can be approximately represented by

$$x(t) = X(t) \sin\{\omega_* t - \theta(t)\} \quad (X \geq 0, 0 \leq \theta < 2\pi), \quad (23)$$

where $X(t)$ is the envelope process of $x(t)$ according to Rice's definition⁽²⁾. Both of $X(t)$, $\theta(t)$ are slow varying functions of time, hence the response velocity can also be represented by

$$\dot{x}(t) = X(t) \omega_* \cos\{\omega_* t - \theta(t)\} \quad (X \geq 0, 0 \leq \theta < 2\pi), \quad (24)$$

Using Eqs. (23), (24), and considering that $\sigma_x^2(t)$, $\sigma_{\dot{x}}^2(t)$ are slow varying functions of time, the following relations are obtained:

$$\left. \begin{aligned} \sigma_x^2(t) &\approx \frac{1}{2} E[X^2], \\ \kappa_{x\dot{x}}(t) &\approx 0, \\ \sigma_{\dot{x}}^2(t) &\approx \frac{\omega_*^2}{2} E[X^2] \approx \omega_*^2 \sigma_x^2(t). \end{aligned} \right\} \quad (25)$$

By virtue of these relations, Eqs (13), (16) become simpler expressions.

The one-time PDF for the envelope can be obtained from the one-time joint PDF of x , \dot{x} given by Eq. (13). Using the technique of transformation of random variables, i.e., transformation from (x, \dot{x}) , to (X, θ) , we can obtain the one-time joint PDF of X , θ . Then, integrating the joint PDF over the θ domain, we have the one-time PDF for the envelope,

$$p(X, t) = \frac{X}{\sigma_x^2(t)} \exp\left\{-\frac{X^2}{2\sigma_x^2(t)}\right\} \quad (X \geq 0). \quad (26)$$

Analogous to Eq. (26), the two-time PDF for the envelope can be obtained from the two-time joint PDF of x , \dot{x} given by Eq. (16), through the transformation of variables from $(x_1, \dot{x}_1; x_2, \dot{x}_2)$ to $(X_1, \theta_1; X_2, \theta_2)$:

$$\begin{aligned} p(X_1, t_1; X_2, t_2) &= \frac{X_1 X_2}{\sigma_x^2(t_1) \sigma_x^2(t_2) \{1 - \eta^2(t_1, t_2)\}} \\ &\times \exp\left\{-\frac{\sigma_x^2(t_2) X_1^2 + \sigma_x^2(t_1) X_2^2}{2\sigma_x^2(t_1) \sigma_x^2(t_2) \{1 - \eta^2(t_1, t_2)\}}\right\} I_0\left(\frac{\eta(t_1, t_2) X_1 X_2}{\sigma_x(t_1) \sigma_x(t_2) \{1 - \eta^2(t_1, t_2)\}}\right), \end{aligned} \quad (27)$$

where I_0 is the modified Bessel function of the zero-th order and $\eta(t_1, t_2)$ is defined by

$$\eta(t_1, t_2) \cong \frac{\sigma_x^2(t_1 \wedge t_2)}{\sigma_x(t_1) \sigma_x(t_2)} e^{-\omega_* |\xi(t_2) - \xi(t_1)|} \quad (28)$$

ANALYSIS OF THE STRUCTURAL RELIABILITY

NONSTATIONARY PROBABILITY DENSITY FUNCTION FOR THE CUMULATIVE DAMAGE OF FATIGUE: The algebraic relation between the tank displacement x and the strain ϵ at a critical portion of the system is assumed to be linear as follows, even though the strain exceeds the range of elasticity:

$$\epsilon = h x \quad (29)$$

Therefore, the virtue of Eq. (23), the amplitude of the strain due to the response of the system can be written as

$$\hat{\epsilon}(t) = h X(t) \quad (30)$$

For the expression of the relation between the strain amplitude, $\hat{\epsilon}$, and the number of cycles to fatigue failure, N_f , the following formula which is proposed by S.S. Manson⁽³⁾ for the low cycle fatigue failure is used here:

$$\hat{\epsilon} = C_0 N_f^{-b_0} \quad (31)$$

where C_0 , b_0 are the material constants.

The cumulative damage based on the Palmgren-Miner theory is considered. According to the theory, the damage accumulated during the period of $[0, t]$ due to the response of the system, $D(t)$, is represented by

$$D(t) = K h^b f_* \int_0^t X^b(\tau) d\tau \quad (32)$$

where

$$b = 1/b_0, \quad K = (1/C_0)^{1/b_0},$$

and where $D(t)$ is approximated by the continuous quantity.

By virtue of Eq. (32), we obtain an expression for the expectation of $D(t)$,

$$\mu_D(t) = K h^b f_* \int_0^t E[X^b(\tau)] d\tau \quad (33)$$

The expectation $E[X^b(\tau)]$ in Eq. (33) can be calculated by employing $p(X, t)$ in Eq. (26). Then,

$$\mu_D(t) = 2^{b/2} \Gamma(b/2 + 1) K h^b f_* \int_0^t \sigma_x^b(\tau) d\tau. \quad (34)$$

Likewise, by virtue of Eq. (32), we obtain an expression for the variance of $D(t)$,

$$\sigma_D^2(t) = (K h^b f_*)^2 \int_0^t \int_0^t E[X^b(\tau_1) X^b(\tau_2)] d\tau_1 d\tau_2 - \mu_D^2(t). \quad (35)$$

It is found that the computation of the variance requires the correlation function $E[X^b(t_1) X^b(t_2)]$, which can be calculated by employing $p(X_1, t_1; X_2, t_2)$ in Eq. (27). Through complicated calculation, the following result is obtained:

$$\sigma_D^2(t) = 2^{b+1} \left\{ \frac{\Gamma(1+b/2)}{\Gamma(b/2)} \right\}^2 (K h^b f_*)^2 \sum_{n=0}^{\infty} \left\{ \left[\frac{\Gamma(n-b/2)}{n!} \right]^2 \int_0^t \frac{\sigma_x^b(\tau_2)}{f_*^n(\tau_2)} \left\{ \int_0^{\tau_2} \sigma_x^b(\tau_1) f_*^n(\tau_1) d\tau_1 \right\} d\tau_2 \right\} - \mu_D^2(t), \quad (36)$$

where

$$g(t) = \sigma_x(t) e^{\omega * \xi(t)}.$$

Though the expectation and the variance of $D(t)$ have been obtained in the theoretical manner as mentioned above, it is difficult to obtain the theoretical distribution of $D(t)$. Then the distribution is assumed to be the log-normal distribution,

$$p(D, t) = \frac{1}{\sqrt{2\pi} D v(t)} \exp \left\{ -\frac{(\ln D - u(t))^2}{2 v^2(t)} \right\} \quad (D \geq 0), \quad (37)$$

where

$$\left. \begin{aligned} u(t) &= \ln \left\{ \frac{\mu_D^2(t)}{\sqrt{\mu_D^2(t) + \sigma_D^2(t)}} \right\}, \\ v^2(t) &= \ln \left\{ \frac{\mu_D^2(t) + \sigma_D^2(t)}{\mu_D^2(t)} \right\}. \end{aligned} \right\} \quad (38)$$

STRUCTURAL RELIABILITY: Let D_M denote the maximum damage accumulated in the material used for the critical portion of the system until fatigue failure. If the Palmgren-Miner theory can be applied in the strict sense, the value of D_M should be the unity. However, it has been shown by experiments that the value of D_M fluctuates. Then we assume that D_M is a random variable and it has the log-normal distribution as well as $D(t)$, i.e.,

$$p(D_M) = \frac{1}{\sqrt{2\pi} D_M v_M} \exp \left\{ -\frac{(\ln D_M - \mu_M)^2}{2 v_M^2} \right\} \quad (D_M \geq 0). \quad (39)$$

The structural reliability from the point of view of fatigue failure is defined as the probability,

$$R(t) = Prob\{D(\tau) < D_u \mid 0 \leq \tau \leq t\} . \quad (40)$$

Since $D(t)$ monotonously increases with time, Eq. (40) can be rewritten as

$$R(t) = Prob\{D(t) < D_u\} . \quad (41)$$

On the other hand, the structural unreliability is defined by

$$F(t) = 1 - R(t) = Prob\{D(t) \geq D_u\} , \quad (42)$$

which indicates the cumulative failure rate during $[0, t]$. On the assumption that $D(t)$ and D_M are statistically independent of each other, $F(t)$ is given by

$$\begin{aligned} F(t) &= \int_0^\infty p(D, t) \left\{ \int_0^\infty p(D_u) dD_u \right\} dD \\ &= \int_0^\infty p(D, t) N\left(\frac{\ln D - u_M}{v_M}\right) dD , \end{aligned} \quad (43)$$

where

$$N(x) = \frac{1}{\sqrt{2\pi}} \int_{-\infty}^x e^{-\xi^2/2} d\xi .$$

Furthermore the failure rate per unit time is given by

$$f(t) = \frac{d}{dt} F(t) = -\frac{d}{dt} R(t) . \quad (44)$$

EXPERIMENTAL AND NUMERICAL RESULTS

Experiments are carried out to examine the analytical results and to obtain the fundamental data, including random excitations of the experimental model with the rectangular tank mentioned before and a fatigue test of supporting legs of the model by sinusoidal excitations.

Figure 7 shows the relation between the tank displacement and the strain at anchored lower ends of the legs in the experimental model. We see that the assumed relation in Eq. (29) is satisfied in this case. Figure 8 shows the observed relation between the strain amplitude at the portions and the number of cycles to the fatigue failure of any one out of four legs of the model subjected to a sinusoidal excitation, from which the material constants in Eq. (31) are obtained for this case.

Figure 9 is a sample of the responses to the random excitations by 264 waves generated from the same population, where the following function is used as $\sqrt{\phi(t)}$;

$$\sqrt{\phi(t)} = e^{-0.125 t} - e^{-0.25 t} \quad (t \geq 0) . \quad (45)$$

In Figs. 10~13, analytical and experimental results for the random responses of the system are shown, and the agreement is satisfactory in Figs. 10, 11, 12. In Fig. 13, the analytical results on the distribution of the cumulative damage due to the response are shown by solid lines. The distribution shown by broken lines is the log-normal distribution having the mean and the variance derived from the experimental data, which agrees well with the distribution by the experiment. This fact means that the assumption on the distribution is reasonable. Therefore, in order to achieve the better agreement between the analytical and the experimental results, the more precise analysis is required for the expectation and, in particular, the variance of the cumulative damage due to the response.

Figure 14 is a numerical example of the structural reliability after 30 seconds from the beginning of excitation versus the maximum (absolute) response acceleration of the system or the maximum power spectrum density (PSD) of the excitation, where the value used for h is about three times as large as the value obtained by the experiment shown in Fig. 7. We can see that the structural reliability rapidly decreases as the maximum acceleration or the maximum PSD increases in the range beyond a certain level. Figure 15 shows the structural reliability, unreliability and the failure rate per unit time varying with time. We found that the reliability is almost determined after 10 seconds in the case where $\sqrt{\phi(t)}$ given by Eq. (45) is used.

ACKNOWLEDGEMENT

This work is carried out as a part of the activity of the EDR research committee. The author would like to express his appreciation to Dr. Prof. H. Shibata, Institute of Industrial Science, University of Tokyo, and the other members of the committee, for their valuable comments.

REFERENCES

- 1) Fujita, T., "Probabilistic Analysis of Response for Nonlinear Systems under Nonstationary Random Excitation", Proc. of 5th Japan Earthquake Eng. Sym.-1978, (Nov. 1978), p.1137, (in Japanese).
- 2) Rice, S.O., "Mathematical Analysis of Random Noise", Reprinted in N. Wax (ed.), "Selected Papers on Noise and Stochastic Processes", Dover, (1954), p.46.

3) Manson, S.S., NACA, TN2933, (1953).

(Manuscript was received on March 24, 1980)

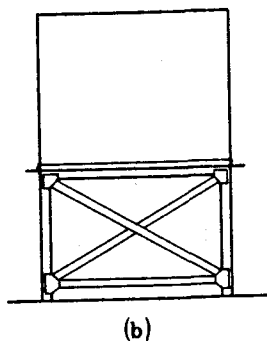
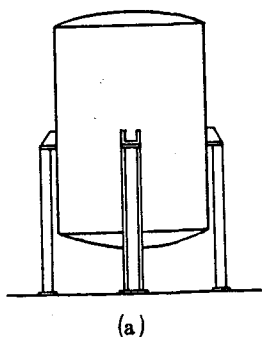


Fig. 1: Examples of leg-supported liquid containers

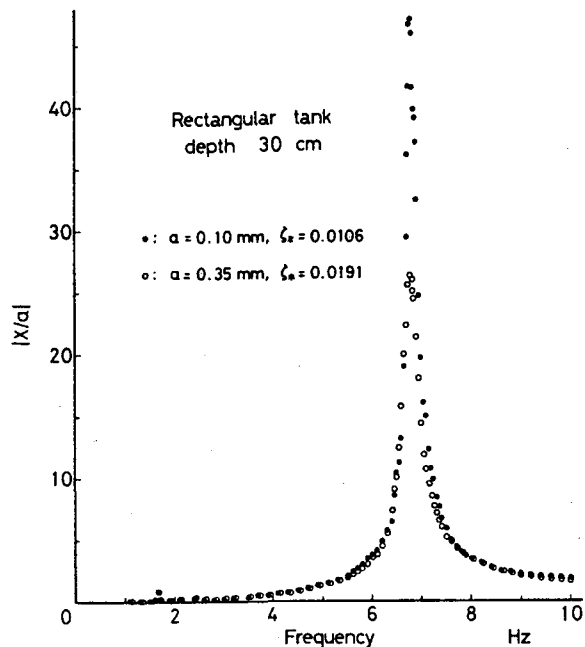


Fig. 2: Response factor on the tank displacement by the experiment

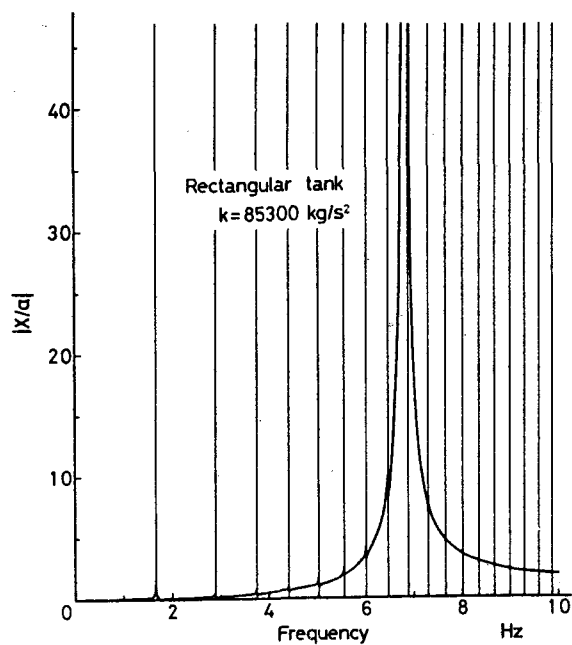


Fig. 3: Response factor on the tank displacement by the potential theory

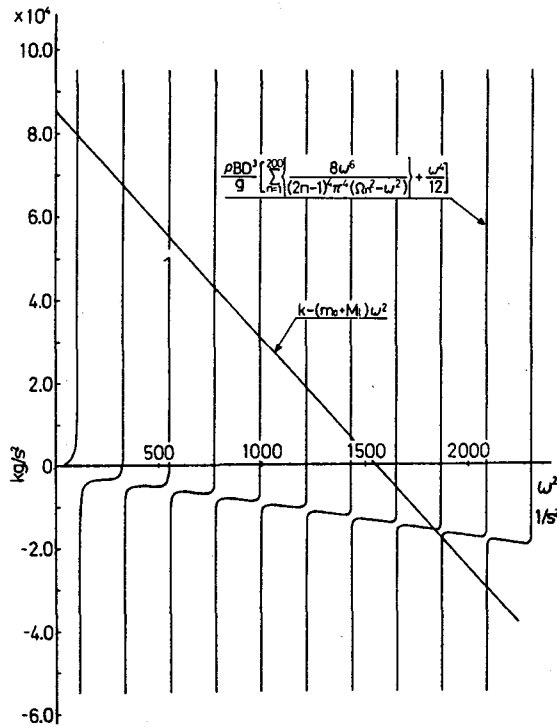


Fig. 4: Graphical solution of the eigen-frequencies

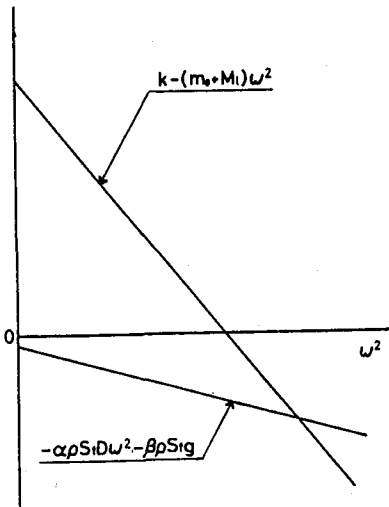


Fig. 5: Simple method for the dominant eigen-frequency

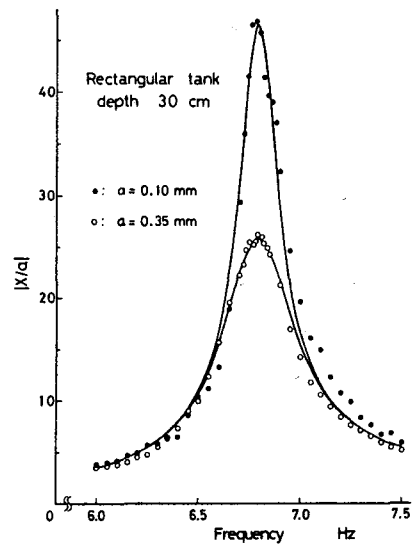


Fig. 6: Response factor on the tank displacement by the non-linear SDF model

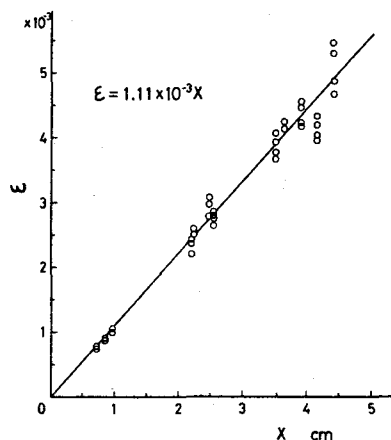


Fig. 7: Tank displacement vs. strain of supporting legs

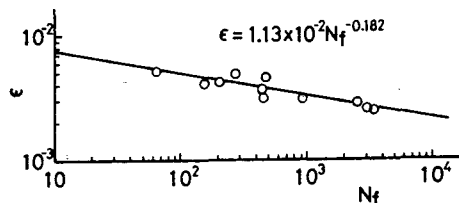


Fig. 8: Strain amplitude vs. number of cycles to the fatigue failure of any one of supporting legs

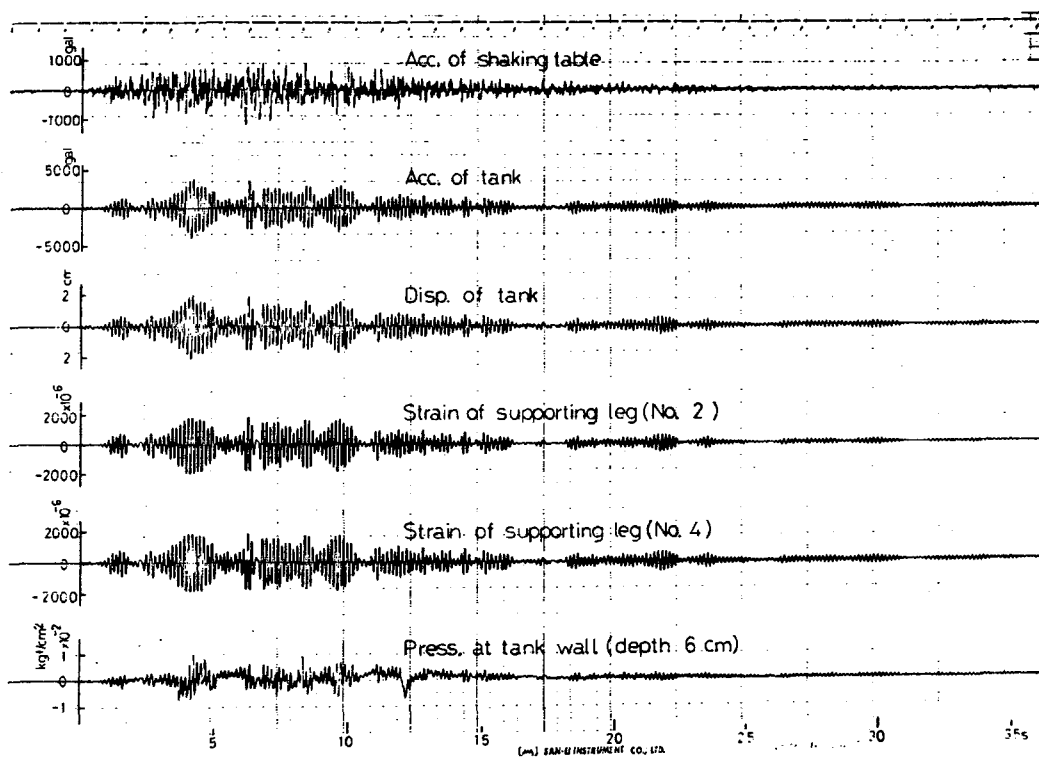


Fig. 9 A sample of the responses to the random excitations

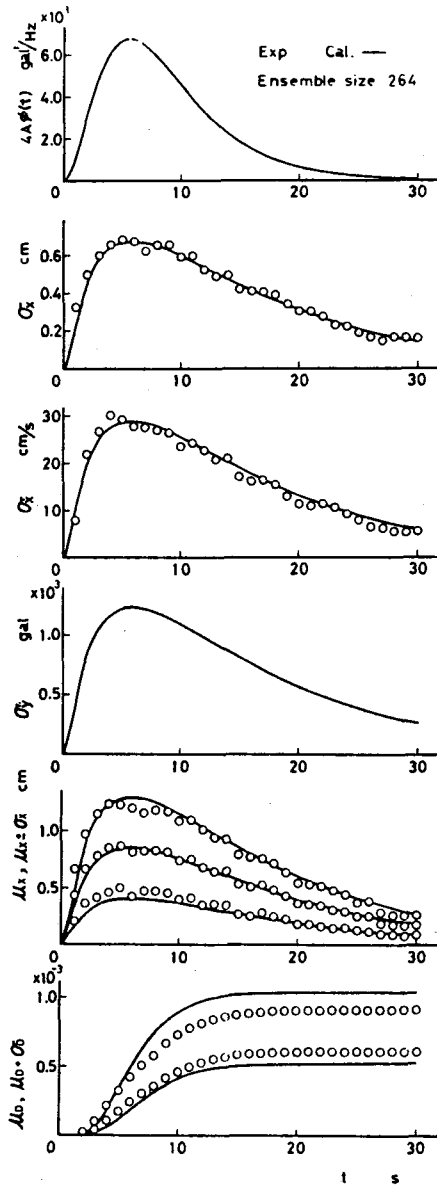


Fig. 10: Nonstationary PSD of the excitation: RMS values of the displacement, velocity and absolute acceleration of the tank; expectations and variances of the envelope and the cumulative damage

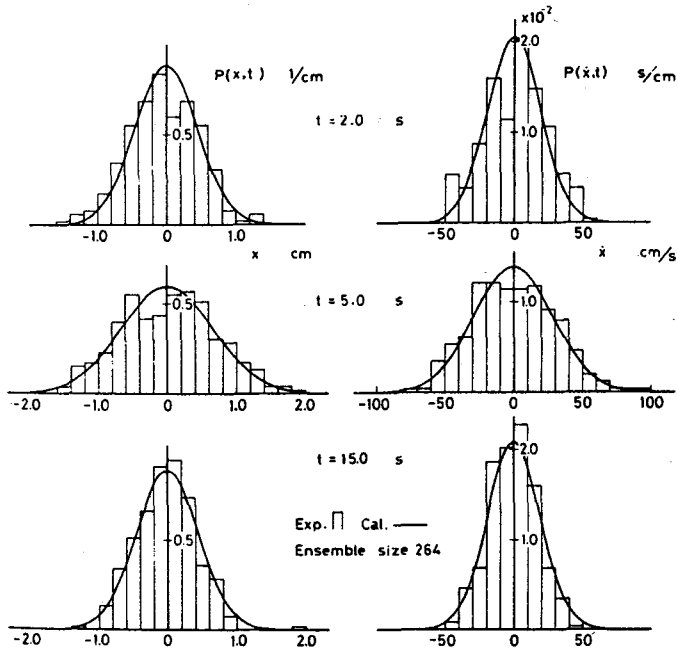


Fig. 11: Nonstationary PDFs of the tank displacement and the tank velocity

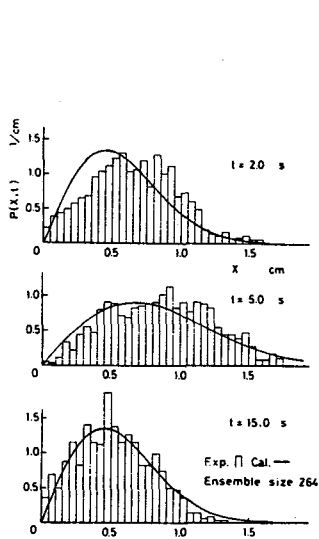


Fig. 12: Nonstationary PDF of the envelope

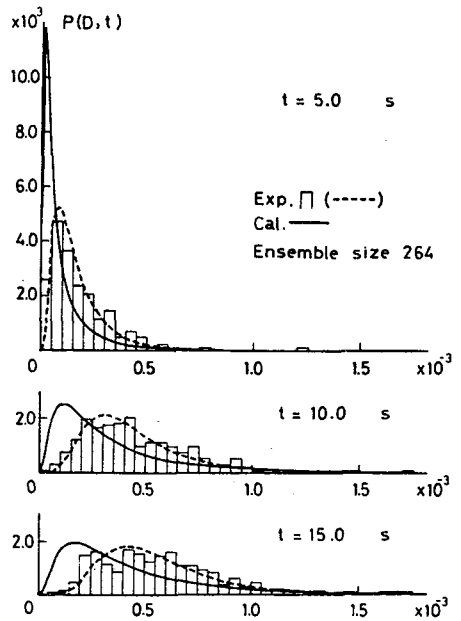


Fig. 13: Nonstationary PDF of the cumulative damage

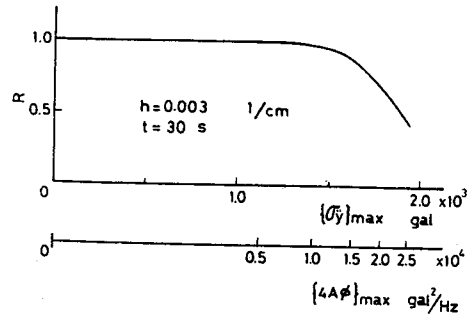


Fig. 14: Structural reliability vs. maximum response acceleration or maximum PSD of the excitation

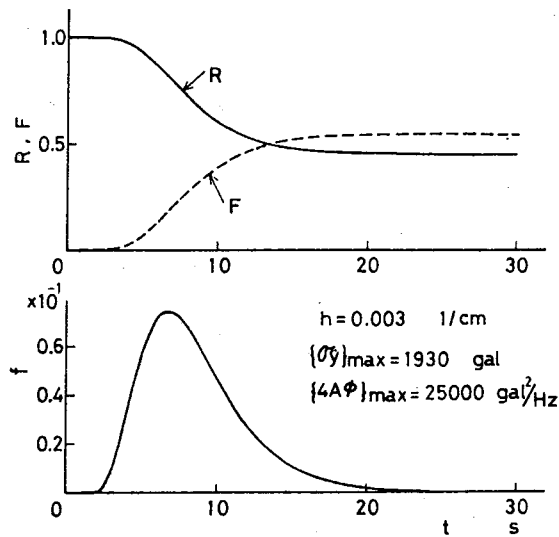


Fig. 15: Structural reliability, unreliability and failure rate per unit time varying with time